

# Pontryagin Optimal Control via Neural Networks

Chengyang Gu, *Student Member, IEEE*, Hui Xiong, *Fellow, IEEE* and Yize Chen, *Member, IEEE*<sup>1</sup>

**Abstract**—Solving real-world optimal control problems are challenging tasks, as the complex, high-dimensional system dynamics are usually unrevealed to the decision maker. It is thus hard to find the optimal control actions numerically. To deal with such modeling and computation challenges, in this paper, we integrate Neural Networks with the Pontryagin’s Maximum Principle (PMP), and propose a sample efficient framework NN-PMP-Gradient. The resulting controller can be implemented for systems with unknown and complex dynamics. By taking an iterative approach, the proposed framework not only utilizes the accurate surrogate models parameterized by neural networks, it also efficiently recovers the optimality conditions along with the optimal action sequences via PMP conditions. Numerical simulations on Linear Quadratic Regulator, energy arbitrage of grid-connected lossy battery, control of single pendulum, and two MuJoCo locomotion tasks demonstrate our proposed NN-PMP-Gradient is a general and versatile computation tool for finding optimal solutions. And compared with the widely applied model-free and model-based reinforcement learning (RL) algorithms, our NN-PMP-Gradient achieves higher sample-efficiency and performance in terms of control objectives.

**Index Terms**—Optimal control; machine learning; neural networks; Pontryagin principle

## I. INTRODUCTION

Solving real-world optimal control problems is possessing huge engineering and societal values, ranging from running power grids, achieving robotics manipulation, and operating transportation networks. However, finding such real-world optimal controllers is often a challenging task, since real-world systems dynamics are usually unrevealed and complex due to their uniqueness, non-linearity and high-dimension [1], [2]. Previous literature provides several extensively utilized approaches on building optimal controllers, including dynamic programming (DP) and model predictive control (MPC) [3]. However, all of these approaches require full knowledge of underlying state transitions. Such restrictions address difficulties on directly applying these approaches in solving complicated real-world optimal control problems with unknown system dynamics [4], [5].

Recent developments of Reinforcement Learning (RL) provides another direction to tackle this problem. Unlike previous model-based approaches, deep RL algorithms relax the requirements over prior knowledge about system dynamics [6]. Instead, agents can be trained to either learn the state-action value function (Q function) or learning the policies directly. Hence, these RL algorithms are termed as *model-free* approaches [7]. Typical deep RL methods achieve

The authors are with the Artificial Intelligence Thrust, Hong Kong University of Science and Technology (Guangzhou), China. Emails: cgu893@connect.hkust-gz.edu.cn, {xionghui, yizechen}@ust.hk .

impressive performances on certain control tasks [8], [9]. However, model-free deep RL methods often suffer from **sample inefficiency**. They usually require huge amount of trials to achieve effective solution, leading to considerable training time, which may also be impractical for real-world applications. Moreover, in general current model-free RL lacks interpretability [10], which raises reliability and safety concerns, especially for problems with hard constraints [11], [12].

To address these challenges, researchers revisit model-based approaches and develop model-based reinforcement learning (MBRL). Such learning-based method usually first acquires a model of system dynamics and then find control policies based on learned models [13]. Recent introduction of deep neural networks (NNs) promises a versatile and efficient modeler for complex, high-dimensional system dynamics [14]. Such surrogate learned models are deployed in model-based RL (MBRL) frameworks [15], [16]. However, typical MBRL algorithms such as MPC with random shooting (RS-MPC) [17] or learning-based policy networks do not provide an explicit mechanism for finding optimal decisions [18]. The lack of tractability severely influence the control performance and reliability of these MBRL algorithms, hence restricting their potential on real-world optimal control problems with unknown dynamics.

In this paper, we design a tractable, sample-efficient MBRL with accurate learnt dynamics model. We start from the idea of learning *complex, unknown system dynamics* with neural networks (NNs) in MBRL. More importantly, we leverage the potential of Pontryagin’s maximum principle (PMP), which offers a theoretical foundation for optimality conditions, and has been used to numerically solve the optimal control actions for a few decades [19]. PMP states a set of necessary conditions, including a minimum condition of the control Hamiltonian, for optimal control policies and optimal state trajectory. Unlike DP or MPC, solving PMP conditions can give the entire optimal solutions over the planning horizon. Working examples on control of electric vehicles [20], supply chain [21], and financial markets [22] have been brought up. Several recent works also considered data-driven design of PMP-based controllers. [23], [24] introduce an auxiliary system by differentiating PMP conditions of given systems, to help take gradients for iteratively updating the parameters of a policy network. In [25] authors directly apply PMP conditions and the Hamiltonian-Jacobian-Bellman (HJB) equations to guide the policy network training. Yet these approaches still require computationally expensive training and solution processes.

Different from previous design of using policy network

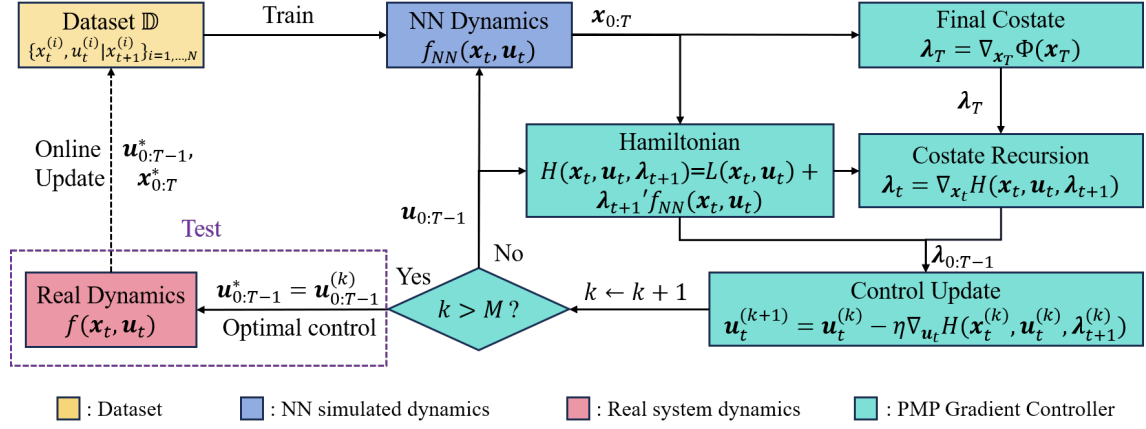


Fig. 1: Schematic of our proposed model learning and control framework based on PMP conditions.

as controller, our major algorithm developed in this work, named **NN-PMP-Gradient**, directly establishes a differentiable algorithm **PMP-Gradient** over PMP conditions to numerically solve the optimal control actions with learned NN system dynamics. We also prove that with accurate NN model, PMP-Gradient controller can at least ensure convergence to local optimal solution, and under certain conditions can converge to global optimal. Numerical simulations on a variety of control tasks including Linear Quadratic Regulator, charging of grid-connected lossy battery, control of single pendulum, and two MuJoCo locomotion, convincingly demonstrate our proposed NN-PMP-Gradient can provide a feasible optimal control. The results also show that our NN-PMP-Gradient: (1) models complex, unknown system dynamics more accurately than traditional Linear models, and hence achieves better control performance. (2) has higher sample efficiency and provide safer solution within state bounds. (3) usually has better control performance than popular model-free RL method PPO, classical model-based RL method RS-MPC, under same learnt NN-dynamics.

## II. PROBLEM FORMULATION

### A. Problem Statement

In this paper, we consider the discrete-time, finite horizon optimal control problem of a dynamical system. For a fixed time horizon  $T$ , we denote the system dynamics as

$$\mathbf{x}_{t+1} = f(\mathbf{x}_t, \mathbf{u}_t), \quad \text{with given } \mathbf{x}_0. \quad (1)$$

Here  $t = 0, 1, 2, \dots, T$  is the time step within the given time horizon.  $\mathbf{x}_t \in \mathbb{R}^m$ ,  $\mathbf{u}_t \in \mathbb{R}^n$  denote the system state and the control variable at time step  $t$  respectively. Eq. (1) is termed as *system dynamics*. In a classic optimal control problem, our goal is to find the optimal control policy  $\pi = \{\mathbf{u}_{0:T-1}^*\}$ , which minimizes the *cost functional*  $J$  under the constraint of system dynamics and given initial state  $\mathbf{x}_0$ :

$$\pi = \arg \min_{\{\mathbf{u}_{0:T-1}\}} J = \Phi(\mathbf{x}_T) + \sum_{t=0}^{T-1} L(\mathbf{x}_t, \mathbf{u}_t) \quad (2)$$

s.t. (1),  $\mathbf{x}_t \in \mathcal{X}, \mathbf{u}_t \in \mathcal{U}$ ;

where  $\mathcal{X} \subseteq \mathbb{R}^n, \mathcal{U} \subseteq \mathbb{R}^m$  represent feasible regions for state and control variables respectively.  $L(\mathbf{x}_t, \mathbf{u}_t)$  denotes *running cost* for each time step, and  $\Phi(\mathbf{x}_T)$  denotes the (optional) *terminal cost* associated with terminal state  $\mathbf{x}_T$ . Without loss of generality, the terminal conditions can be treated either as a constraint or as a penalty term in  $\Phi(\cdot)$ . Also note  $L(\cdot)$  and  $\Phi(\cdot)$  are usually artificially designated functions.

In this work, we know the decision maker knows the exact function form of control objectives. Normally, with known, linear system dynamics, we can resort to off-the-shelf optimization solvers like convex optimization solver or MPC approaches to find the sequence of optimal actions  $\mathbf{u}_{0:T-1}^*$ . However, in many real-world cases, system dynamics are highly non-linear and unrevealed to controllers, such like the robot locomotion models in robotic control tasks or battery chemical degradation models in the battery energy management tasks. Such situation makes these classic techniques less effective and not readily applicable. This motivates us to explore novel optimal control frameworks.

### B. Pontryagin Maximum Principle

In this Subsection, we recall (discrete-time) Pontryagin's Maximum Principle (PMP) [19], which offers a set of necessary conditions that the optimal trajectory  $\{\mathbf{x}_{0:T}^*, \mathbf{u}_{0:T-1}^*\}$  must satisfy in the optimal control problem Eq. (2). To introduce these necessary conditions, we write the *Hamiltonian*:

$$H(\mathbf{x}_t, \mathbf{u}_t, \lambda_{t+1}) = L(\mathbf{x}_t, \mathbf{u}_t) + \lambda_{t+1}' f(\mathbf{x}_t, \mathbf{u}_t); \quad (3)$$

where  $\lambda_t$  is named as *costate* with  $\lambda_t'$  as its transpose. Based on PMP conditions, at time step  $t$  in the horizon  $[0, T-1]$  the optimal control  $\mathbf{u}_t^*$  must satisfy the following conditions:

$$\lambda_t^* = \frac{\partial H(\mathbf{x}_t^*, \mathbf{u}_t^*, \lambda_{t+1}^*)}{\partial \mathbf{x}_t^*}; \quad (4)$$

$$\lambda_T^* = \frac{\partial \Phi(\mathbf{x}_T^*)}{\partial \mathbf{x}_T^*}; \quad (5)$$

$$\frac{\partial H(\mathbf{x}_t^*, \mathbf{u}_t^*, \lambda_{t+1}^*)}{\partial \mathbf{u}_t^*} = 0. \quad (6)$$

Eq. (4)-(6) are termed as *PMP Conditions*. We refer to [26] for the proof of PMP on standard discrete-time system

(2). Essentially, PMP conditions characterize the first-order conditions around the optimality for all kinds of systems. By directly solving PMP conditions Eq. (4)-(6), or integrating them into other algorithm blocks, we can overcome the failure of classical convex solver on complex non-linear systems. However, this still requires full information of the control Hamiltonian along its first-order information with respect to both state variables and control variables. Yet in many real-world applications,  $H(\mathbf{x}_t^*, \mathbf{u}_t^*, \lambda_{t+1}^*)$  may not be revealed to engineers or decision makers, or only partial of the dynamics information are available. Moreover, previous attempts on using PMP conditions for finding closed-form solutions of the optimal controller only work with limited form of dynamics or cost functions [20]. This motivates us to examine how to integrate data-driven dynamical model into PMP conditions, and investigate the computational method to solve for  $\mathbf{u}_t^*$ .

### III. MODEL-BASED OPTIMAL CONTROLLER DESIGN

In this section, we demonstrate our proposed model-based approach for optimal control named **NN-PMP-Gradient**, which is composed of two major parts: i). train neural networks (NN) to learn system dynamics offline from data; and ii). use a PMP-based gradient method to obtain the optimal control policy based on the learned dynamics. Proposed scheme of NN-PMP-Gradient is illustrated in Fig. 1.

#### A. System Identification with Neural Networks

We would like to leverage PMP's advantages on finding optimal control sequences, while the system dynamics are unknown. To realize it, we first need an effective method to identify the unrevealed system dynamics, since applying PMP requires the explicit expression of system dynamics. In our proposed approach, we utilize the function approximation capabilities of NN, and parameterize the system dynamics either wholly or partially as a neural network:

$$\mathbf{x}_{t+1} = f_{NN}(\mathbf{x}_t, \mathbf{u}_t) \quad \text{with given } \mathbf{x}_0; \quad (7)$$

Usually we train the NN-simulated system dynamics  $f_{NN}$  offline with dataset  $\mathbb{D} = \{\mathbf{x}_t^{(i)}, \mathbf{u}_t^{(i)} | \mathbf{x}_{t+1}^{(i)}\}_{i=1,2,\dots,N}$ . To establish  $\mathbb{D}$ , we randomly collected state-control pairs  $\{\mathbf{x}_t^{(i)}, \mathbf{u}_t^{(i)}\}$  from state and control space  $\mathcal{X}, \mathcal{U}$  as features, and use ground-truth system dynamics  $f$  to generate next state  $\mathbf{x}_{t+1}^{(i)}$  as supervised labels. Once the training data is collected, we use mean squared error (MSE) to train  $f_{NN}$ :

$$\mathcal{L}_{sysid} = \frac{1}{N} \sum_{i=1}^N (\mathbf{x}_{t+1}^{(i)} - f_{NN}(\mathbf{x}_t^{(i)}, \mathbf{u}_t^{(i)}))^2. \quad (8)$$

To improve the dynamics approximation accuracy, we can also train  $f_{NN}$  in an online fashion by updating  $\mathbb{D}$  with new state-control pairs executed in the control process and re-training  $f_{NN}$ , which is also broadly used in the Reinforcement Learning community. Based on the trained system dynamics and designated optimizing objective, we formulate the Hamiltonian and establish equations for optimal control and state trajectory with PMP Conditions Eq.

(4)-(6). However, as non-linearity shows up in NN-simulated system dynamics  $f_{NN}$ , we still face challenges in directly solving these equations, which motivates us to find numerical way to solve these equations with learned dynamics involved.

#### B. PMP-Gradient Controller Design

With dynamics accurately parameterized by the learned function  $f_{NN}$  in Eq. (7), we are able to establish PMP conditions Eq. (4)-(6) for the system. While the ultimate goal is to find solutions for these equations, which help us get the optimal control policy  $\pi = \mathbf{u}_{0:T-1}^*$  of the sequential decision-making problems. Due to the non-linearity and complicated function space of  $f_{NN}$ , it is challenging to directly obtain solutions in an analytical way. To overcome the difficulty, we design a gradient-based method named **PMP-Gradient**, to compute the numerical value of  $\pi$ .

In this approach, we start from an initialized random control policy  $\mathbf{u}_{0:T-1}^{(1)}$ , and use it to retrieve corresponding state sequence  $\mathbf{x}_{0:T}^{(1)}$  based on NN-simulated system dynamics Eq. (7). Then based on it, we recursively compute costate  $\lambda_{0:T}^{(1)}$  with PMP Conditions Eq. (4)-(5):

$$\begin{aligned} \lambda_T^{(1)} &= \frac{\partial \Phi(\mathbf{x}_T^{(1)})}{\partial \mathbf{x}_T^{(1)}}; \\ \lambda_t^{(1)} &= \frac{\partial H(\mathbf{x}_t^{(1)}, \mathbf{u}_t^{(1)}, \lambda_{t+1}^{(1)})}{\partial \mathbf{x}_t^{(1)}}. \end{aligned} \quad (9)$$

Based on values of obtained states and costates, we update controls by taking gradients of Hamiltonian  $H(\mathbf{x}_t^{(1)}, \mathbf{u}_t^{(1)}, \lambda_{t+1}^{(1)})$  w.r.t.  $\mathbf{u}_t^{(1)}$  and apply a gradient descent optimizer with learning rate  $\eta$  to update  $\mathbf{u}_t^{(2)}$ :

$$\mathbf{u}_t^{(2)} = \mathbf{u}_t^{(1)} - \eta \frac{\partial H(\mathbf{x}_t^{(1)}, \mathbf{u}_t^{(1)}, \lambda_{t+1}^{(1)})}{\partial \mathbf{u}_t^{(1)}}, \quad t \in [0, T]. \quad (10)$$

By repeating the above process until maximum iterations  $M$ , we iteratively update control policy  $\mathbf{u}_{0:T-1}$  to reach solutions of PMP Condition Eq. (6). The full algorithm is illustrated in Algorithm 1.

Essentially, we utilize a fully differentiable procedure by using the learned dynamics  $f_{NN}$  with the corresponding Hamiltonian and the terminal cost. When  $f_{NN}$  approximates ground-truth  $f$  accurately, we have the following Lemma regarding step 5 – 6 of PMP-Gradient Algorithm 1 and Theorem for cost  $J$  in optimal control problem Eq. (2):

*Lemma 1:* Implementing Eq. (10) is equivalent to taking gradient descent step  $\mathbf{u}_t^{(k+1)} = \mathbf{u}_t^{(k)} - \eta \frac{\partial J}{\partial \mathbf{u}_t^{(k)}}$ .

*Theorem 2:* Suppose Objective  $J$  is differentiable and strictly convex with respect to  $\mathbf{u}_t^{(k)}$ , and  $\frac{\partial J}{\partial \mathbf{u}_t^{(k)}}$  is Lipschitz Continuous with constant  $L > 0$ . Then gradient descent  $\mathbf{u}_t^{(k+1)} = \mathbf{u}_t^{(k)} - \eta \frac{\partial J}{\partial \mathbf{u}_t^{(k)}}$  guarantees global optimal with learning rate  $\eta \leq 1/L$ .

Based on Lemma 1 and Theorem 2, we can infer that our PMP-Gradient Controller has global convergence guarantees with convergence rate  $O(1/\eta)$  when  $J$  is a convex function w.r.t. control variable  $\mathbf{u}_t$  for all  $t = 0, 1, \dots, T-1$  (and

	$T$	$(m, n)$	Running Cost $L(\mathbf{x}_t, \mathbf{u}_t)$	Terminal Cost $\Phi(\mathbf{x}_T)$	System Dynamics $f(\mathbf{x}_t, \mathbf{u}_t)$
LQR	10	(5, 3)	$\mathbf{x}_t' \mathbf{Q} \mathbf{x}_t + \mathbf{u}_t' \mathbf{R} \mathbf{u}_t$	$\mathbf{x}_T' \mathbf{Q} \mathbf{x}_T$	$\mathbf{A} \mathbf{x}_t + \mathbf{B} \mathbf{u}_t$
Battery	24	(1, 1)	$p_t \mathbf{u}_t + \alpha \mathbf{u}_t^2 + P_e(\mathbf{x}_t)$	$\gamma(\mathbf{x}_T - \mathbf{x}_f)^2$	$\zeta(\mathbf{u}_t) \mathbf{u}_t + \mathbf{x}_t$
Pendulum	10	(2, 1)	$w_q(q_t - q_f)^2 + w_{dq}(dq_t - dq_f)^2 + w_u \mathbf{u}_t^2$	$w_q(q_T - q_f)^2 + w_{dq}(dq_T - dq_f)^2$	$\mathbf{x}_t + \Delta[dq_t, \frac{u_t - mg \sin(q_t)}{I}]'$
Swimmer	500	(10, 2)	$w_c \mathbf{u}_t \mathbf{u}_t$	$w_f(\mathbf{x}_0[0] - \mathbf{x}_T[0])$	unknown
HalfCheetah	500	(18, 6)	$w_c \mathbf{u}_t \mathbf{u}_t$	$w_f(\mathbf{x}_0[0] - \mathbf{x}_T[0])$	unknown

TABLE I: Settings of testing environments. For Swimmer and HalfCheetah we do not know the exact formulation of the system dynamics, and all algorithms need to learn the dynamics or policy.

### Algorithm 1 PMP-Gradient Controller

**Require:** Initial state  $\mathbf{x}_0$ ; Maximum iterations  $M$ ; Learning rate  $\eta$ ; NN-simulated system dynamics  $\mathbf{x}_{t+1} = f_{NN}(\mathbf{x}_t, \mathbf{u}_t)$ ;

**Require:** Running cost  $L(\mathbf{x}_t, \mathbf{u}_t)$ ; Terminal cost  $\Phi(\mathbf{x}_T)$ .

- 1:  $k = 1$ .
- 2: Initialize control policy  $\mathbf{u}_{0:T-1}^{(1)}$ .
- 3: **while**  $k \leq M$  **do**
- 4:     Compute  $\mathbf{x}_{0:T}^{(k)}$  with current control policy  $\mathbf{u}_{0:T-1}^{(k)}$ , based on  $\mathbf{x}_{t+1} = f_{NN}(\mathbf{x}_t, \mathbf{u}_t)$  and  $\mathbf{x}_0$ .
- 5:     Compute terminal costate  $\lambda_T^{(k)}$  by  $\lambda_T^{(k)} = \frac{\partial \Phi(\mathbf{x}_T^{(k)})}{\partial \mathbf{x}_T^{(k)}}$ .
- 6:     Compute costate  $\lambda_t^{(k)}$  for  $t = 0, 1, \dots, T-1$ , based on  $\lambda_t^{(k)} = \frac{\partial H(\mathbf{x}_t^{(k)}, \mathbf{u}_t^{(k)}, \lambda_{t+1}^{(k)})}{\partial \mathbf{x}_t^{(k)}}$  and  $\lambda_T^{(k)}$ .
- 7:     Update Control Policy:  $\mathbf{u}_t^{(k+1)} \leftarrow \mathbf{u}_t^{(k+1)} - \eta \frac{\partial H(\mathbf{x}_t^{(k)}, \mathbf{u}_t^{(k)}, \lambda_{t+1}^{(k)})}{\partial \mathbf{u}_t^{(k)}}$ .
- 8:      $k \leftarrow k + 1$
- 9: **end while**
- 10:  $\mathbf{u}_{0:T-1}^* \leftarrow \mathbf{u}_{0:T-1}^{(k)}$

has at least local convergence guarantees for general cases). The proof of Lemma 1 and Theorem 2 can be found in Appendix A in our paper’s online version [27]. To accelerate convergence process, we can also apply other gradient-based optimizer like conjugate gradient (CG) optimizer, Newton’s method to replace gradient descent in step 7 in Algorithm 1.

Different from directly performing gradient descent over objective  $J$ , our PMP-Gradient controller has no need to consider terms with future states  $\mathbf{x}_{t+1:T}$  when taking derivatives of  $H(\mathbf{x}_t, \mathbf{u}_t, \lambda_{t+1})$  w.r.t.  $\mathbf{u}_t$ . This helps us eliminate computations of Hessian matrices  $\frac{\partial \mathbf{x}_{t+1}}{\partial \mathbf{x}_t}$ , hence reducing the size of computation graph for calculating gradients and greatly improving the computation time. For problems with hard state and action bounds, we modify objective and step 7 in Algorithm 1. Detailed settings can be found in Appendix B in our paper’s online version [27].

### IV. NUMERICAL EXAMPLES

In this section, we evaluate the optimal control performance of our proposed NN-PMP-Gradient controller and illustrate its versatile capabilities on numerical simulations of 5 tasks. In simulations we benchmark against: i). a Linear-Convex solver, which we firstly use linear regression to approximate a linearized system dynamics and then solve optimal control problem using cvxpy solver [28]; ii). state-of-the-art model-free RL algorithm Proximal Policy Optimization (PPO); and iii). model-based random shooting MPC (RS-MPC) controller (based on NN-simulated system

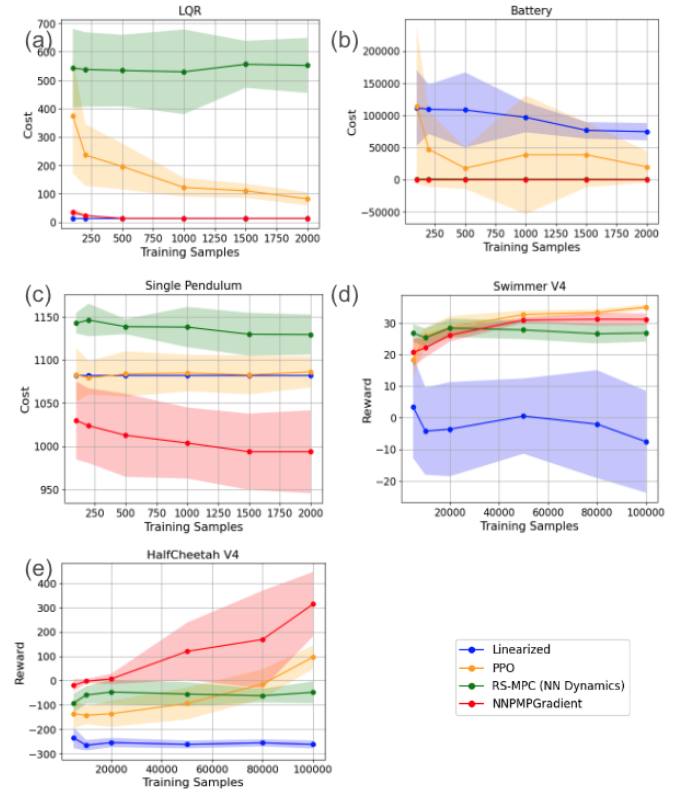


Fig. 2: Sample-Performance (Cost/Reward) curves on 5 different experiment environments. (a) LQR (Cost); (b) Battery (Cost); (c) Pendulum (Cost); (d) MuJoCo Swimmer (Reward); (e) MuJoCo HalfCheetah (Reward).

dynamics) [17]. To benchmark performances, for all simulations we use a Google Colab T4 GPU with 12GB RAM.

#### A. Experiment Control Tasks

In this subsection, we briefly introduce 5 optimal control environments for our experiment. The settings of each task (including time horizon  $T$ , state and action dimension  $m, n$ , running cost  $L(\mathbf{x}_t, \mathbf{u}_t)$ , terminal cost  $\Phi(\mathbf{x}_T)$  and system dynamics  $f(\mathbf{x}_t, \mathbf{u}_t)$ ) is illustrated in Table I. We note that in all test cases, it is assumed that the ground truth dynamics are not revealed to the controller. Detailed settings of these systems can be found in Appendix C in our paper’s online version [27].

**1. Linear Quadratic Regulator (LQR).** In this case, we set up a finite-horizon Linear Quadratic Regulator (LQR) model with 5 states and 3 actions with choice of stabilizable ( $A, B$ ).

**2. Battery.** We consider optimal arbitrage of a battery. The battery make profits via participating in electricity markets and making charging or discharging decisions under time-varying prices. A profitable energy storage arbitrage plan is crucial, since it encourages utilization of stochastic renewables and addressing energy sustainability [29]. The battery has a nonlinear and unknown charging efficiency with respect to battery’s state-of-charge.

**3. Pendulum.** We consider controlling a single pendulum system, where control variable  $\mathbf{u}_t$  denotes the applied torque, while the 2-dimension state  $[q_t, dq_t]'$  include angular velocity  $q_t$  and angular acceleration  $dq_t$ .

**4. MuJoCo Swimmer.** We consider the control of MuJoCo robot Swimmer [30]. The problem involves a 2-dimension control variable  $\mathbf{u}_t$  and a 10-dimension state  $\mathbf{x}_t$ . The first element of state  $\mathbf{x}_t[0]$  denotes the robot’s x-coordinate. For optimal control, we want the Swimmer robot to move forward along x-axis as much as possible with small control cost.  $w_c$  and  $w_f$  are cost weights.

**5. MuJoCo HalfCheetah.** This problem involves a 6-dimension control variable  $\mathbf{u}_t$  and a 18-dimension state  $\mathbf{x}_t$ . The control objective is same as Swimmer.

### B. Numerical Results

We evaluate the performance of our proposed NN-PMP-Gradient on the 5 tasks mentioned in Section IV-A. For LQR, Single Pendulum, Swimmer and HalfCheetah experiments, we apply neural network  $f_{NN}$  to learn the full system dynamics  $f(\mathbf{x}_t, \mathbf{u}_t)$ , while in Battery case we use  $f_{NN}$  to learn part of the dynamics: the charging efficiency function  $\zeta(\mathbf{u}_t)$ . In all 5 experiments, we compare our NN-PMP-Gradient method against Linearized model, classic model-free RL method PPO and model-based RL method RS-MPC (based on the same NN-simulated system dynamics in our NN-PMP-Gradient method). For all environments tested we find NN-PMP-Gradient converges during policy inference.

Table. II shows the control performance of each control method across all 5 experiments. In general, the results demonstrate that our NN-PMP-Gradient outperforms Linearized model, PPO, and RS-MPC in terms of control performance using same number of training samples. For example, in Single Pendulum experiment, with NN-dynamics trained by 2,000 samples, our NN-PMP-Gradient reduces the cost by at least 90 compared with Linearized model, PPO and RS-MPC, yielding more than 8.2% improvement; while in HalfCheetah case, with NN-dynamics trained by 100,000 samples, our method shows more than 200 leading in reward, which is huge improvement compared to the best result 96.73 (achieved by PPO) among the rest 3 methods. We also note that in specific cases with strong local optima like Swimmer [31], though NN-PMP-Gradient still achieves competitive control performance, lack of random search may add difficulty for escaping from local optima, making it underperform model-free PPO with a very narrow gap. Meanwhile, the inaccuracy when using NN to approximate complex, high-dimension system dynamics like HalfCheetah, causes bigger variances in NN-PMP-Gradient’s control performance. We

regard such observations as limitations of our method, and will address them in the future work.

Fig. 2 illustrates the control performance trend of each method as the training samples increase. We find our NN-PMP-Gradient keeps a considerable leading in control performance. In most cases, even with significantly fewer training samples for learning the system dynamics, our method still achieves comparable results with higher reward/lower costs.

	Linearized	PPO	RS-MPC	Ours
<b>SBER</b>	54.3% $\pm$ 2.3%	33.7% $\pm$ 21.3%	5.1% $\pm$ 1.4%	0.0% $\pm$ 0.0%

TABLE III: State Bounds Exceeding Rates (SBER) on the Battery experiment. Results are averaged for 3 runs (each contains 10 trials).

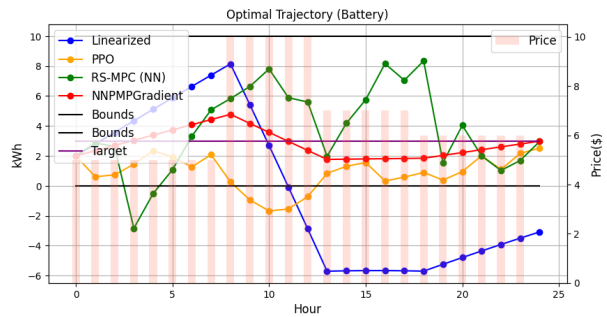


Fig. 3: A State Trajectory Example in Battery experiment. Only trajectory obtained by NN-PMP-Gradient does not exceed state bounds, while others does.

Furthermore, simulation results highlight advantages of our NN-PMP-Gradient on satisfying safety constraints for control problems defined by the state or action constraints. In the Battery case, Table. III shows the average State Bounds Exceeding Rate (SBER) in battery experiment with 2,000 training samples, which records the proportion of state trajectories that exceed bounds obtained by various controllers across total time steps. Fig. 3 shows one-day state trajectory comparison for the Battery case. We can observe only our method constrains the battery state-of-charge within the pre-defined 0 – 10 kWh limits, while other algorithms’ resulting actions cause the battery to be easily overdischarged with state-of-charge smaller than 0 kWh. More importantly, we can observe our proposed algorithm can charge the battery when price is lower, while selling power at hours with higher price during noon. These results further indicate that our NN-PMP-Gradient yields safer and realistic solutions, and hence improves the control performance significantly.

### V. CONCLUSION AND DISCUSSION

In this paper, we showed that the classic theories of optimal control, the Pontryagin’s Principle, can be seamlessly integrated into data-driven settings. The proposed NN-PMP-Gradient is able to both accurately simulate and optimally control unknown dynamical systems. Simulations on five numerical examples (LQR, battery, single pendulum, MuJoCo

	LQR	Battery	Pendulum	Swimmer	HalfCheetah
Linearized	13.43 $\pm$ 0.00	74581.94 $\pm$ 13446.32	1081.97 $\pm$ 0.00	-7.61 $\pm$ 0.37	-261.44 $\pm$ 16.45
PPO	82.48 $\pm$ 23.12	19619.10 $\pm$ 24318.00	1086.11 $\pm$ 18.14	34.99 $\pm$ 0.85	96.73 $\pm$ 47.00
RS-MPC	552.31 $\pm$ 96.98	300.23 $\pm$ 206.92	1129.46 $\pm$ 23.23	26.81 $\pm$ 2.72	-47.62 $\pm$ 44.77
<b>Ours</b>	13.53 $\pm$ 0.09	-3.20 $\pm$ 0.00	993.53 $\pm$ 48.08	31.12 $\pm$ 1.85	313.77 $\pm$ 131.96
Number of Samples	2,000	2,000	2,000	100,000	100,000

TABLE II: Performances under varying training samples, according to the complexity of experiment environments. The performances are averaged for 10 runs test. For LQR, Battery and Pendulum the control performance is evaluated by control costs (the lower the better); for Swimmer and HalfCheetah we evaluate the accumulated reward (the higher the better).

Swimmer and HalfCheetah) demonstrated our NN-PMP-Gradient outperforms standard optimization-based solver using linearized dynamics, model-free PPO and model-based RS-MPC under a variety of settings. For complex real-world systems, the proposed method is a more sample-efficient, generalizable and safer optimal controller.

There exist several limitations to the current PMP-based data-driven control scheme. The current method can be affected by modeling errors during NN training, which causes high variances in control performance for high-dimensional systems like MuJoCo HalfCheetah. Additionally, for some specific scenarios with strong local optima like Swimmer, lack of random search limits proposed method’s performance. Moreover, for problems with long horizon and high dimension, the co-state recursion in PMP-Gradient can impose high computational burden. In the future, we aim to address these challenges and seek theoretical insights to enhance our NN-PMP-Gradient as a more robust and efficient model-based optimal controller.

## REFERENCES

- [1] R. S. Sutton, A. G. Barto, and R. J. Williams, “Reinforcement learning is direct adaptive optimal control,” *IEEE control systems magazine*, vol. 12, no. 2, pp. 19–22, 1992.
- [2] W. Jin *et al.*, “Learning from sparse demonstrations,” *IEEE Transactions on Robotics*, 2022.
- [3] R. Bellman, “Dynamic programming,” *Science*, vol. 153, no. 3731, pp. 34–37, 1966.
- [4] F. L. Lewis, D. Vrabie, and V. L. Syrmos, *Optimal control*. John Wiley & Sons, 2012.
- [5] Y. Wang and S. Boyd, “Fast model predictive control using online optimization,” *IEEE Transactions on control systems technology*, vol. 18, no. 2, pp. 267–278, 2009.
- [6] R. S. Sutton and A. G. Barto, *Reinforcement Learning: An Introduction*, 2nd ed. The MIT Press, 2018. [Online]. Available: <http://incompleteideas.net/book/the-book-2nd.html>
- [7] I. Koryakovskiy, M. Kudruss, R. Babuška, W. Caarls, C. Kirches, K. Mombaur, J. P. Schlöder, and H. Vallery, “Benchmarking model-free and model-based optimal control,” *Robotics and Autonomous Systems*, vol. 92, pp. 81–90, 2017.
- [8] V. Mnih, K. Kavukcuoglu, D. Silver, A. Graves, I. Antonoglou, D. Wierstra, and M. Riedmiller, “Playing atari with deep reinforcement learning,” *arXiv preprint arXiv:1312.5602*, 2013.
- [9] T. P. Lillicrap, J. J. Hunt, A. Pritzel, N. Heess, T. Erez, Y. Tassa, D. Silver, and D. Wierstra, “Continuous control with deep reinforcement learning,” *arXiv preprint arXiv:1509.02971*, 2015.
- [10] A. Verma, V. Murali, R. Singh, P. Kohli, and S. Chaudhuri, “Programmatically interpretable reinforcement learning,” in *International Conference on Machine Learning*. PMLR, 2018, pp. 5045–5054.
- [11] J. Garcia and F. Fernández, “A comprehensive survey on safe reinforcement learning,” *Journal of Machine Learning Research*, vol. 16, no. 1, pp. 1437–1480, 2015.
- [12] M. Zanon and S. Gros, “Safe reinforcement learning using robust mpc,” *IEEE Transactions on Automatic Control*, 2021.
- [13] C. Atkeson and J. Santamaria, “A comparison of direct and model-based reinforcement learning,” in *Proceedings of International Conference on Robotics and Automation*, vol. 4, 1997, pp. 3557–3564.
- [14] A. Nagabandi, G. Kahn, R. S. Fearing, and S. Levine, “Neural network dynamics for model-based deep reinforcement learning with model-free fine-tuning,” in *2018 IEEE International Conference on Robotics and Automation (ICRA)*, 2018, pp. 7559–7566.
- [15] S. Levine and V. Koltun, “Learning complex neural network policies with trajectory optimization,” in *Proceedings of the 31st International Conference on Machine Learning*, vol. 32, no. 2. PMLR, 2014.
- [16] Y. Chen, Y. Shi, and B. Zhang, “Optimal control via neural networks: A convex approach,” in *International Conference on Learning Representations*, 2019.
- [17] A. Nagabandi, G. Kahn, R. S. Fearing, and S. Levine, “Neural network dynamics for model-based deep reinforcement learning with model-free fine-tuning,” in *2018 IEEE International Conference on Robotics and Automation (ICRA)*. IEEE, 2018, pp. 7559–7566.
- [18] T. Dinev, C. Mastalli, V. Ivan, S. Tonneau, and S. Vijayakumar, “Differentiable optimal control via differential dynamic programming,” *arXiv preprint arXiv:2209.01117*, 2022.
- [19] L. S. Pontryagin, *Mathematical theory of optimal processes*. CRC press, 1987.
- [20] N. R. Chowdhury, R. Ofir, N. Zargari, D. Baimel, J. Belikov, and Y. Levron, “Optimal control of lossy energy storage systems with nonlinear efficiency based on dynamic programming and pontryagin’s minimum principle,” *IEEE Transactions on Energy Conversion*, vol. 36, no. 1, pp. 524–533, 2020.
- [21] D. Ivanov and B. Sokolov, “Dynamic supply chain scheduling,” *Journal of scheduling*, vol. 15, no. 2, pp. 201–216, 2012.
- [22] G. Wang and Z. Yu, “A pontryagin’s maximum principle for non-zero sum differential games of bdes with applications,” *IEEE Transactions on Automatic control*, vol. 55, no. 7, pp. 1742–1747, 2010.
- [23] W. Jin, Z. Wang, Z. Yang, and S. Mou, “Pontryagin differentiable programming: An end-to-end learning and control framework,” *Advances in Neural Information Processing Systems*, vol. 33, 2020.
- [24] L. Böttcher, N. Antulov-Fantulin, and T. Asikis, “Ai pontryagin or how artificial neural networks learn to control dynamical systems,” *Nature communications*, vol. 13, no. 1, p. 333, 2022.
- [25] S. Engin and V. Isler, “Neural optimal control using learned system dynamics,” *arXiv preprint arXiv:2302.09846*, 2023.
- [26] A. E. Bryson and Y.-C. Ho, *Applied optimal control: optimization, estimation, and control*. Routledge, 2018.
- [27] C. Gu, X. Hui, and Y. Chen, “Pontryagin optimal control via neural networks,” *Online Preprint Version, arXiv:2212.14566*, 2022.
- [28] S. Diamond and S. Boyd, “Cvxpy: A python-embedded modeling language for convex optimization,” *The Journal of Machine Learning Research*, vol. 17, no. 1, pp. 2909–2913, 2016.
- [29] R. M. Dell and D. A. J. Rand, “Energy storage—a key technology for global energy sustainability,” *Journal of power sources*, vol. 100, no. 1-2, pp. 2–17, 2001.
- [30] E. Todorov, T. Erez, and Y. Tassa, “Mujoco: A physics engine for model-based control,” in *2012 IEEE/RSJ International Conference on Intelligent Robots and Systems*. IEEE, 2012, pp. 5026–5033.
- [31] M. Franceschetti, C. Lacoux, R. Ohouens, A. Raffin, and O. Sigaud, “Making reinforcement learning work on swimmer,” *arXiv preprint arXiv:2208.07587*, 2022.
- [32] K. Khamaru and M. Wainwright, “Convergence guarantees for a class of non-convex and non-smooth optimization problems,” in *International Conference on Machine Learning*. PMLR, 2018.
- [33] J. D. Lee, M. Simchowitz, M. I. Jordan, and B. Recht, “Gradient descent only converges to minimizers,” in *Conference on learning theory*. PMLR, 2016, pp. 1246–1257.

## APPENDIX

### A. Convergence Proof of PMP-Gradient Controller

**Lemma 1.** Implementing Eq. (10) is equivalent to taking gradient descent step  $\mathbf{u}_t^{(k+1)} = \mathbf{u}_t^{(k)} - \eta \frac{\partial J}{\partial \mathbf{u}_t^{(k)}}$ .

*Proof:* Recall the formulation of Hamiltonian  $H(\mathbf{x}_t, \mathbf{u}_t, \lambda_{t+1})$  is:

$$H(\mathbf{x}_t, \mathbf{u}_t, \lambda_{t+1}) = L(\mathbf{x}_t, \mathbf{u}_t) + \lambda_{t+1}' f(\mathbf{x}_t, \mathbf{u}_t); \quad (11)$$

Based on Eq. (11) and PMP Conditions we get:

$$\begin{aligned} \lambda_T^{(k)} &= \frac{\partial \Phi(\mathbf{x}_T^{(k)})}{\partial \mathbf{x}_T^{(k)}} \\ \lambda_t^{(k)} &= \frac{\partial H(\mathbf{x}_t^{(k)}, \mathbf{u}_t^{(k)}, \lambda_{t+1}^{(k)})}{\partial \mathbf{x}_t^{(k)}} \\ &= \frac{\partial L(\mathbf{x}_t^{(k)}, \mathbf{u}_t^{(k)})}{\partial \mathbf{x}_t^{(k)}} + \lambda_{t+1}^{(k)} \frac{\partial f(\mathbf{x}_t^{(k)}, \mathbf{u}_t^{(k)})}{\partial \mathbf{x}_t^{(k)}} \end{aligned} \quad (12)$$

Notice that:

$$f(\mathbf{x}_t^{(k)}, \mathbf{u}_t^{(k)}) = \mathbf{x}_{t+1}^{(k)} \quad (13)$$

Hence, we have:

$$\begin{aligned} \lambda_{T-1}^{(k)} &= \frac{\partial L(\mathbf{x}_{T-1}^{(k)}, \mathbf{u}_{T-1}^{(k)})}{\partial \mathbf{x}_{T-1}^{(k)}} + \lambda_T^{(k)} \frac{\partial \mathbf{x}_T^{(k)}}{\partial \mathbf{x}_{T-1}^{(k)}} \\ &= \frac{\partial L(\mathbf{x}_{T-1}^{(k)}, \mathbf{u}_{T-1}^{(k)})}{\partial \mathbf{x}_{T-1}^{(k)}} + \frac{\partial \Phi(\mathbf{x}_T^{(k)})}{\partial \mathbf{x}_T^{(k)}} \frac{\partial \mathbf{x}_T^{(k)}}{\partial \mathbf{x}_{T-1}^{(k)}} \\ &= \frac{\partial L(\mathbf{x}_{T-1}^{(k)}, \mathbf{u}_{T-1}^{(k)})}{\partial \mathbf{x}_{T-1}^{(k)}} + \frac{\partial \Phi(\mathbf{x}_T^{(k)})}{\partial \mathbf{x}_{T-1}^{(k)}} \end{aligned} \quad (14)$$

Based on Eq. (12) and Eq. (14) do the recursion:

$$\lambda_t^{(k)} = \begin{cases} \sum_{i=t}^{T-1} \left( \frac{\partial L(\mathbf{x}_i^{(k)}, \mathbf{u}_i^{(k)})}{\partial \mathbf{x}_i^{(k)}} \right) + \frac{\partial \Phi(\mathbf{x}_T^{(k)})}{\partial \mathbf{x}_T^{(k)}} & 0 \leq t \leq T-1, \\ \frac{\partial \Phi(\mathbf{x}_T^{(k)})}{\partial \mathbf{x}_T^{(k)}} & t = T. \end{cases} \quad (15)$$

Based on Eq. (15) we compute  $\frac{\partial H}{\partial \mathbf{u}_t^{(k)}}$  ( $0 \leq t \leq T-1$ ):

$$\begin{aligned} \frac{\partial H}{\partial \mathbf{u}_t^{(k)}} &= \frac{\partial L(\mathbf{x}_t^{(k)}, \mathbf{u}_t^{(k)})}{\partial \mathbf{u}_t^{(k)}} + \lambda_{t+1}^{(k)} \frac{\partial \mathbf{x}_{t+1}^{(k)}}{\partial \mathbf{u}_t^{(k)}} \\ &= \frac{\partial L(\mathbf{x}_t^{(k)}, \mathbf{u}_t^{(k)})}{\partial \mathbf{u}_t^{(k)}} + \sum_{i=t+1}^{T-1} \left( \frac{\partial L(\mathbf{x}_i^{(k)}, \mathbf{u}_i^{(k)})}{\partial \mathbf{u}_i^{(k)}} \right) + \frac{\partial \Phi(\mathbf{x}_T^{(k)})}{\partial \mathbf{u}_t^{(k)}} \\ &= \sum_{i=t}^{T-1} \left( \frac{\partial L(\mathbf{x}_i^{(k)}, \mathbf{u}_i^{(k)})}{\partial \mathbf{u}_i^{(k)}} \right) + \frac{\partial \Phi(\mathbf{x}_T^{(k)})}{\partial \mathbf{u}_t^{(k)}} \end{aligned} \quad (16)$$

According to Eq. (2) we compute  $\frac{\partial J}{\partial \mathbf{u}_t^{(k)}}$ :

$$\frac{\partial J}{\partial \mathbf{u}_t^{(k)}} = \frac{\partial (\sum_{t=0}^{T-1} L(\mathbf{x}_t^{(k)}, \mathbf{u}_t^{(k)}) + \Phi(\mathbf{x}_T^{(k)}))}{\partial \mathbf{u}_t^{(k)}} \quad (17)$$

Notice that:

$$\frac{\partial (\sum_{i=0}^{t-1} L(\mathbf{x}_i^{(k)}, \mathbf{u}_i^{(k)}))}{\partial \mathbf{u}_t^{(k)}} = 0 \quad (18)$$

Hence we have

$$\frac{\partial J}{\partial \mathbf{u}_t^{(k)}} = \sum_{i=t}^{T-1} \left( \frac{\partial L(\mathbf{x}_i^{(k)}, \mathbf{u}_i^{(k)})}{\partial \mathbf{u}_i^{(k)}} \right) + \frac{\partial \Phi(\mathbf{x}_T^{(k)})}{\partial \mathbf{u}_t^{(k)}} \quad (19)$$

Compare Eq. (16) with Eq. (19), we have:

$$\frac{\partial J}{\partial \mathbf{u}_t^{(k)}} = \frac{\partial H}{\partial \mathbf{u}_t^{(k)}} \quad (20)$$

Hence, PMP Gradient Controller  $\mathbf{u}_t^{(k+1)} \leftarrow \mathbf{u}_t^{(k+1)} - \eta \frac{\partial H(\mathbf{x}_t^{(k)}, \mathbf{u}_t^{(k)}, \lambda_{t+1}^{(k)})}{\partial \mathbf{x}_t^{(k)}}$  is equivalent to gradient descent  $\mathbf{u}_t^{(k+1)} = \mathbf{u}_t^{(k)} - \eta \frac{\partial J}{\partial \mathbf{u}_t^{(k)}}$ .  $\blacksquare$

**Theorem 2.** Suppose Objective  $J$  is a *differentiable and convex function w.r.t  $\mathbf{u}_t^{(k)}$* , and  $\frac{\partial J}{\partial \mathbf{u}_t^{(k)}}$  is *Lipschitz Continuous* with constant  $L > 0$ . Then gradient descent  $\mathbf{u}_t^{(k+1)} = \mathbf{u}_t^{(k)} - \eta \frac{\partial J}{\partial \mathbf{u}_t^{(k)}}$  guarantees global optimal with learning rate  $\eta \leq 1/L$ .

*Proof:* Since  $\frac{\partial J}{\partial \mathbf{u}_t^{(k)}}$  is *Lipschitz Continuous*, we have:

$$J(\mathbf{y}) = J(\mathbf{z}) + \frac{\partial J}{\partial \mathbf{z}}(\mathbf{y} - \mathbf{z}) + \frac{1}{2}L\|\mathbf{y} - \mathbf{z}\|_2^2 \quad (21)$$

Let  $\mathbf{z} = \mathbf{u}_t^{(k)}$ ,  $\mathbf{y} = \mathbf{u}_t^{(k)} - \eta \frac{\partial J}{\partial \mathbf{u}_t^{(k)}}$ :

$$\begin{aligned} J(\mathbf{u}_t^{(k)} - \eta \frac{\partial J}{\partial \mathbf{u}_t^{(k)}}) &= J(\mathbf{u}_t^{(k)}) - \eta \|\frac{\partial J}{\partial \mathbf{u}_t^{(k)}}\|_2^2 + \frac{1}{2}L\|\eta \frac{\partial J}{\partial \mathbf{u}_t^{(k)}}\|_2^2 \\ &= J(\mathbf{u}_t^{(k)}) - (\eta - \frac{1}{2}L\eta^2)\|\frac{\partial J}{\partial \mathbf{u}_t^{(k)}}\|_2^2 \end{aligned} \quad (22)$$

Since  $0 < \eta \leq 1/L$ ,  $\eta - \frac{1}{2}L\eta^2 > 0$ , we have:

$$J(\mathbf{u}_t^{(k)} - \eta \frac{\partial J}{\partial \mathbf{u}_t^{(k)}}) < J(\mathbf{u}_t^{(k)}) \quad (23)$$

Hence, the gradient descent will decrease. Now we prove it will converge to global optimal solution  $\mathbf{u}_t^*$ . Since  $J$  is convex w.r.t  $\mathbf{u}_t^{(k)}$ , we have:

$$J(\mathbf{u}_t^{(k)}) \leq J(\mathbf{u}_t^*) + \frac{\partial J}{\partial \mathbf{u}_t^{(k)}}(\mathbf{u}_t^{(k)} - \mathbf{u}_t^*) \quad (24)$$

Plug Eq. (22) in. And consider  $0 \leq L \leq 1/\eta$ ,  $\eta - \frac{1}{2}L\eta^2 \geq \frac{1}{2}\eta$ :

$$\begin{aligned} J(\mathbf{u}_t^{(k)} - \eta \frac{\partial J}{\partial \mathbf{u}_t^{(k)}}) &\leq J(\mathbf{u}_t^{(k)}) - \frac{1}{2}\eta \|\frac{\partial J}{\partial \mathbf{u}_t^{(k)}}\|_2^2 \\ &\leq J(\mathbf{u}_t^*) + \frac{\partial J}{\partial \mathbf{u}_t^{(k)}}(\mathbf{u}_t^{(k)} - \mathbf{u}_t^*) - \frac{1}{2}\eta \|\frac{\partial J}{\partial \mathbf{u}_t^{(k)}}\|_2^2 \end{aligned} \quad (25)$$

Reform Eq. (25):

$$\begin{aligned} J(\mathbf{u}_t^{(k)} - \eta \frac{\partial J}{\partial \mathbf{u}_t^{(k)}}) - J(\mathbf{u}_t^*) & \\ &\leq \frac{1}{2\eta}(\|\mathbf{u}_t^{(k)} - \mathbf{u}_t^*\|_2^2 - \|\mathbf{u}_t^{(k)} - \mathbf{u}_t^* - \eta \frac{\partial J}{\partial \mathbf{u}_t^{(k)}}\|_2^2) \end{aligned} \quad (26)$$

Summation over iterations:

$$\begin{aligned} & \sum_{i=0}^{k-1} (J(\mathbf{u}_t^{(i)}) - \eta \frac{\partial J}{\partial \mathbf{u}_t^{(i)}}) - J(\mathbf{u}_t^*) \\ & \leq \sum_{i=0}^{k-1} \left( \frac{1}{2\eta} (\|\mathbf{u}_t^{(i)} - \mathbf{u}_t^*\|_2^2 - \|\mathbf{u}_t^{(i+1)} - \mathbf{u}_t^*\|_2^2) \right) \\ & \leq \frac{1}{2\eta} \|\mathbf{u}_t^{(0)} - \mathbf{u}_t^*\|_2^2 \end{aligned} \quad (27)$$

Since  $J(\mathbf{u}_t^{(k)} - \eta \frac{\partial J}{\partial \mathbf{u}_t^{(k)}}) = J(\mathbf{u}_t^{(k+1)}) < J(\mathbf{u}_t^{(k)})$ , we have:

$$\begin{aligned} J(\mathbf{u}_t^{(k)}) - J(\mathbf{u}_t^*) & \leq \frac{1}{k} \sum_{i=0}^{k-1} (J(\mathbf{u}_t^{(i)}) - \eta \frac{\partial J}{\partial \mathbf{u}_t^{(i)}}) - J(\mathbf{u}_t^*) \\ & \leq \frac{1}{2\eta k} \|\mathbf{u}_t^{(0)} - \mathbf{u}_t^*\|_2^2. \end{aligned} \quad (28)$$

Eq. (28) implies the convergence to global optimal solution  $\mathbf{u}_t^*$  with rate  $O(1/\eta)$ .  $\blacksquare$

*Theorem 2* shows the global convergence of gradient descent over objective  $J$  when  $J$  is convex w.r.t control  $\mathbf{u}_t^{(k)}$ . Since *Lemma 1* holds, it also proves the global convergence of PMP Gradient controller (Algorithm. 1). Further studies imply that for some special non-convex function  $J$  (e.g. satisfying *Kurdyka-Łojasiewicz* Inequalities [32]) gradient descent (and hence PMP Gradient Controller) will also converge to global optimal, and it is proved that they are unlikely be trapped in saddle points [33]. For other common non-convex cases, PMP Gradient Controller will only converge to local optimal.

### B. Settings of NN-PMP-Gradient for Problems with State and Action Bounds

For optimal control problems with action bounds  $\underline{u}, \bar{u}$  ( $\underline{u}$ : lower bound,  $\bar{u}$ : upper bound), we check the updated control action in Algorithm 1 at each iteration  $k$ :

$$\mathbf{u}_t^{(k+1)} \leftarrow \mathbf{u}_t^{(k+1)} - \eta \frac{\partial H(\mathbf{x}_t^{(k)}, \mathbf{u}_t^{(k)}, \lambda_{t+1}^{(k)})}{\partial \mathbf{u}_t^{(k)}} \quad (29)$$

Let  $\mathbf{u}_t^{(k+1)}[i]$  denote element  $i$  of obtained  $\mathbf{u}_t^{(k+1)}$ . We set:

$$\mathbf{u}_t^{(k+1)}[i] \leftarrow \begin{cases} \bar{u} - \theta & \text{if } \mathbf{u}_t^{(k+1)}[i] \geq \bar{u}; \\ \underline{u} + \theta & \text{if } \mathbf{u}_t^{(k+1)}[i] \leq \underline{u}; \\ \text{unchanged,} & \text{else;} \end{cases} \quad (30)$$

for each elements  $i$  of  $\mathbf{u}_t^{(k+1)}$  to ensure it is within bounds.  $\theta$  is a small value. We set it to be  $10^{-6}$  in our experiments.

For optimal control problems with state bounds  $\underline{x}, \bar{x}$  ( $\underline{x}$ : lower bound,  $\bar{x}$ : upper bound), we add an extra quadratic penalty term  $P_e(\mathbf{x}_t)$  in the running cost  $L(\mathbf{x}_t, \mathbf{u}_t)$ :

$$P_e(\mathbf{x}_t) = \begin{cases} \sum_{i=1}^m \beta(\mathbf{x}_t[i] - \underline{x})^2 & \mathbf{x}_t[i] < \underline{x}, \\ 0 & 0 \leq \mathbf{x}_t \leq \bar{x}, \\ \sum_{i=1}^m \beta(\mathbf{x}_t[i] - \bar{x})^2 & \bar{x} < \mathbf{x}_t[i]. \end{cases} \quad (31)$$

In the above penalty formulation,  $\mathbf{x}_t[i]$  denotes element  $i$  of  $\mathbf{x}_t$ .  $m$  is the dimension of  $\mathbf{x}_t$  and  $\beta$  is the penalty coefficient. The penalty term  $P_e$  generates huge cost when any element of  $\mathbf{x}_t$  exceeds state bounds, serving as soft constraints for state variable  $\mathbf{x}_t$ .

### C. Detailed Settings of Experiment Environments

#### Environment 1: Linear Quadratic Regulator (LQR)

Linear Quadratic Regulator (LQR) is a classical problem in optimal control theory. It has linear system dynamics and quadratic cost. A standard finite-horizon LQR can be formulated as:

$$\begin{aligned} \min_{\{\mathbf{u}_{0:T-1}\}} \quad & \sum_{t=0}^{T-1} (\mathbf{x}_t' \mathbf{Q} \mathbf{x}_t + \mathbf{u}_t' \mathbf{R} \mathbf{u}_t) + \mathbf{x}_T' \mathbf{Q}_T \mathbf{x}_T \\ \text{s.t.} \quad & \mathbf{x}_{t+1} = \mathbf{A} \mathbf{x}_t + \mathbf{B} \mathbf{u}_t. \end{aligned} \quad (32)$$

where  $\mathbf{Q}$ ,  $\mathbf{R}$  and  $\mathbf{Q}_T$  are *positive semi-definite* matrices. In our experiment, we set  $\mathbf{Q}$  and  $\mathbf{A}$  to be identity matrices with dimension 5,  $\mathbf{R}$  to be identity matrix with dimension 3, and

$$\mathbf{Q}_T = \begin{bmatrix} 5 & 0 & 0 & 0 & 0 \\ 0 & 4 & 0 & 0 & 0 \\ 0 & 0 & 2 & 0 & 0 \\ 0 & 0 & 0 & 1 & 0 \\ 0 & 0 & 0 & 0 & 3 \end{bmatrix}, \quad \mathbf{B} = \begin{bmatrix} 1 & 0 & 0 \\ 0 & 1 & 0 \\ 0 & 0 & 1 \\ 1 & 1 & 0 \\ 0 & 1 & 1 \end{bmatrix} \quad (33)$$

#### Environment 2: Battery

The optimal control task of Battery system involves a 1-dimensional control variable  $\mathbf{u}_t$  ( $\underline{u} \leq \mathbf{u}_t \leq \bar{u}$ ), which represents the amount of electricity charged or discharged at time step  $t$ ; and a 1-dimensional state  $\mathbf{x}_t$ , which represents the remaining battery electricity. The running cost consists of three components: (1) charging cost  $p_t \mathbf{u}_t$  (where  $p_t$  is the time-varying grid electricity selling price) (2) penalty for excessive (dis)charging amount  $\mathbf{u}_t$ :  $\alpha \mathbf{u}_t^2$  (3) penalty term  $P_e(\mathbf{x}_t)$  as soft constraint to prevent  $\mathbf{x}_t$  from exceeding the battery capacity limit  $\bar{x}$ :

$$P_e(\mathbf{x}_t) = \begin{cases} \beta x_t^2 & x_t < 0, \\ 0 & 0 \leq x_t \leq \bar{x}, \\ \beta(x_t - \bar{x})^2 & \bar{x} < x_t. \end{cases} \quad (34)$$

Terminal cost  $\gamma(\mathbf{x}_T - \mathbf{x}_f)^2$  penalizes deviations from target final state  $\mathbf{x}_f$ . For battery systems, there exists a non-linear charging efficiency term related to battery's charging level (state-of-charge). Considering the loss in charging/discharging process, the system dynamics is defines as:

$$\mathbf{x}_{t+1} = \zeta(\mathbf{u}_t) \mathbf{u}_t + \mathbf{x}_t; \quad (35)$$

where  $\zeta(\mathbf{u}_t)$  denotes the non-linear charging efficiency function w.r.t  $\mathbf{u}_t$ . In the simulation, we use a nonlinear function  $\zeta(\mathbf{u}_t) = 0.5 + \frac{1}{1+e^{\mathbf{u}_t}}$ . We note that such battery's charging efficiency function is not known explicitly by the users or controller, thus it is appropriate to use a neural network to approximate such dynamics (35).

The full formulation of the optimal control problem is:

$$\begin{aligned} \min_{\{\mathbf{u}_{0:T-1}\}} \sum_{t=0}^{T-1} & (p_t \mathbf{u}_t + \alpha \mathbf{u}_t^2 + P_e(\mathbf{x}_t)) + \gamma (\mathbf{x}_T - \mathbf{x}_f)^2 \\ \text{s.t. } & x_{t+1} = \zeta(\mathbf{u}_t) \mathbf{u}_t + \mathbf{x}_t \end{aligned} \quad (36)$$

### Environment 3: Pendulum

For optimal control of Single Pendulum System, control variable  $\mathbf{u}_t$  denotes the applied torque, while the 2-dimension state  $[q_t, dq_t]'$  includes angular velocity  $q_t$  and angular acceleration  $dq_t$ .

Our objective is to minimize the summation of squared errors between  $q_t$  and target  $q_f$ ,  $dq_t$  and target  $dq_f$ , and the square value of control torque  $\mathbf{u}_t$  within time horizon:

$$\begin{aligned} \min_{\{\mathbf{u}_{0:T-1}\}} \sum_{t=0}^{T-1} & (w_q(q_t - q_f)^2 + w_{dq}(dq_t - dq_f)^2 + w_u \mathbf{u}_t^2) \\ & + w_q(q_T - q_f)^2 + w_{dq}(dq_T - dq_f)^2 \\ \text{s.t. } & x_{t+1} = f(\mathbf{x}_t, \mathbf{u}_t) \end{aligned} \quad (37)$$

In the above formulation,  $w_q$ ,  $w_{dq}$ ,  $w_u$  are cost weights. The system dynamics  $f(\mathbf{x}_t, \mathbf{u}_t)$  is established following the *Newton's Second Law of Rotation*:

$$f(\mathbf{x}_t, \mathbf{u}_t) = \mathbf{x}_t + \Delta \left[ dq_t, \frac{u_t - mglq_t - \sigma \sin(q_t)}{I} \right]'; \quad (38)$$

where  $m$  and  $l$  denotes mass and length of the pendulum;  $g$  is the gravity constant;  $I = \frac{1}{3}mgl^2$  is the pendulum's moment of inertia;  $\Delta$  is the time step length; and  $\sigma$  is the damping ratio.